Analytica Chimica Acta 1175 (2021) 338734

Contents lists available at ScienceDirect

Analytica Chimica Acta

journal homepage: www.elsevier.com/locate/aca

A novel disease-associated nucleic acid sensing platform based on split DNA-scaffolded sliver nanocluster

Zhenzhen Jia [a, b], Kangsheng Tu [c], Qiuran Xu [d], Wenhui Gao [a, b], Cui Liu [a, b], Biyun Fang [a, b, *], Mingzhen Zhang [a, b, **]

[a] School of Basic Medical Sciences, Xi'an Key Laboratory of Immune Related Diseases, Xi'an Jiaotong University, Xi'an, Shaanxi, 710061, China
[b] Key Laboratory of Environment and Genes Related to Diseases, Xi'an Jiaotong University, Ministry of Education, Xi'an, Shaanxi, 710061, China
[c] Department of Hepatobiliary Surgery, The First Affiliated Hospital of Xi'an Jiaotong University, Xi'an, Shaanxi, 710061, China
[d] The Key Laboratory of Tumor Molecular Diagnosis and Individualized Medicine of Zhejiang Province, Zhejiang Provincial People's Hospital, Affiliated People's Hospital, Hangzhou Medical College, Hangzhou, 310014, China

HIGHLIGHTS

- Disease-associated nucleic acids detection based on split DNA scaffold-Ag NC was proposed.
- The methods for miR-362 or hDNA detection showed good sensitivity, selectivity, and practicability.
- This one-step assay method has advantages of rapid, economy and easy to operation.

GRAPHICAL ABSTRACT

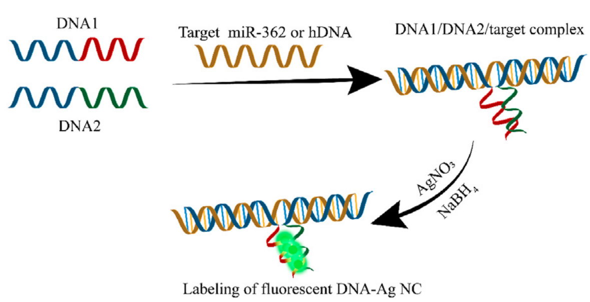

ARTICLE INFO

Article history:
Received 6 April 2021
Received in revised form
1 May 2021
Accepted 1 June 2021
Available online 7 June 2021

Keywords:
DNA-sliver nanocluster
Fluorescence probe
Nucleic acid
Biosensor

ABSTRACT

Disease-associated nucleic acids, such as DNAs and miRNAs, are important biomarkers for the diagnosis, prognosis and treatment guidance of human diseases. Therefore, the accurate and sensitive detection of nucleic acid is of great significance for the early diagnosis of diseases. DNA-scaffolded silver nanocluster (DNA-Ag NC) is a new type of probe with good photostability and low toxicity that has been widely used in biomedical analysis. In this work, a new universal sensing platform based on target triggered labeling luminescent DNA-Ag NC for disease-related nucleic acids detection was constructed. The assembled split DNA fragment pair (C_4AC_4T and C_3GT_4) could be used as a template to develop a bright green fluorescent Ag NC. According to this phenomenon, we devised two probe sequences DNA 1 and DNA 2, which could hybridize to the same one target and contained a different split fragment of Ag NC' scaffold. The target compelled the split fragments close to each other through base pairing with DNA 1 and DNA 2, thus quantification of the target could be achieved through measuring green fluorescence of Ag NC that produced by assembled scaffold in ternary hybrid products. We applied this platform successfully for miR-362, a potential biomarker of inflammatory bowel diseases (IBD), or HIV-related DNA (hDNA) detection, achieving the detection limits of 6.5 nM and 1.7 nM, respectively. Both of the assays showed excellent reproducibility, selectivity and potential applications in human serum samples. In summary, an

* Corresponding author. School of Basic Medical Sciences, Xi'an Key Laboratory of Immune Related Diseases, Xi'an Jiaotong University, Xi'an, Shaanxi, 710061, China.
** Corresponding author. School of Basic Medical Sciences, Xi'an Key Laboratory of Immune Related Diseases, Xi'an Jiaotong University, Xi'an, Shaanxi, 710061, China.
E-mail addresses: byfang89@xjtu.edu.cn (B. Fang), mzhang21@xjtu.edu.cn (M. Zhang).

https://doi.org/10.1016/j.aca.2021.338734

economic and convenient universal platform was developed for disease-associated nucleic acid detection.

1. Introduction

Nucleic acids are natural biopolymers of nucleotides that store, encode, transmit and express genetic information. Both DNA sequence and RNA transcripts play crucial roles in diverse biological events, which can be exploited to serve as biomarkers for biological studies and clinical diagnosis [1]. Traditional methods for nucleic acids assay such as polymerase chain reaction [2], Northern blotting [3], and oligonucleotide microarrays [4], have been demonstrated with good sensitivity and selectivity, however, the time-consuming and high-cost limit their wide range of applications [5,6]. Therefore, it is a major requirement to develop cost-effective, simple, accurate, and sensitive methods for nucleic acid quantification.

There are numerous methods have been developed for nucleic acids quantification, such as fluorescence [7], electrochemistry [8], Raman spectroscopy [9,10], colorimetry [11,12]. Among them, the fluorescent method is in dominant place because of its high sensitivity and selectivity, simple operation, and fast response process. Recently, DNA templated silver nanoclusters (DNA-Ag NC) with significant advantages has become a new class of biosensing and imaging fluorophores. Besides of small size [13], excellent photostability [14], good biocompatibility [15,16], easy preparation [17], it also has the followed prominent advantages. First, the spectra and photophysics of Ag NC are strongly influenced by DNA structure/sequence. DNA strands with different sequences determine cluster size, geometry and electronic structure [18,19]. Thus, Ag NCs' color and brightness are drastically altered by different DNA templated sequences or by hybridization with single-stranded oligonucleotides [20–23]. The fluorescence switchable property of DNA-Ag NC could be used as a new signal transformation mode for biosensors. For example, Fang et al. found that the fluorescence of DNA-Ag NC could be quenched by its complementary oligonucleotides, then they developed a strategy for target miRNA detection through restoring the quenched fluorescence of Ag NC based on strands exchange reaction [24]. Second, DNA-based Ag NC fluorophores were easy to fabricate sensors [25–30]. Zhou et al. constructed an aptamer-tagged DNA-Ag NC for Mucin1 detection. The specific binding of Mucin1 to its aptamer affected the conformation of the aptamer, resulting in the fluorescence change of the DNA-Ag NC [25]. Therefore, DNA-Ag NC would be a substitutable fluorescent material to fabricate biosensors for the detection of target nucleic acids.

According to Dickson's report [31], DNA fragment pair (C_4AC_4T and C_3GT_4) as an Ag NC scaffold could also develop the same bright green fluorescent Ag NC that formed by the parent $C_4AC_4TC_3GT_4$ sequence. In this paper, we used this phenomenon as signal output to develop a facile, label-free and universal fluorescence assay platform for target nucleic acid detection. The probe contained two DNA sequences, DNA1 and DNA2, which were partly complementary to the target and contained a different split fragment of Ag NC's scaffold respectively. The formed DNA1/DNA2/target ternary complex would compel the two split DNA fragments close to each other through base pairing, so the target nucleic acid could be analyzed quantitatively by measuring fluorescence intensity of the synthesized silver nanocluster. The assays for target microRNA-362 (miR-362), a potential biomarker in inflammatory bowel disease (IBD) [32,33], and target HIV-related DNA (hDNA) [34] were respectively developed and verified, which would provide a reference for designing assays for other nucleotides by using this target-triggered labeling split DNA-Ag NC method.

2. Experimental section

2.1. Instrument

The fluorescence spectra of the prepared DNA-templated Ag NCs were recorded by a fluorescence spectrophotometer (HITACHI-F4700, JP). The transmission electron microscopy (JEOL JEM-2100, JP) was used to characterize the morphology of the Ag NC. The hydrated size and potential of the silver clusters were measured on the Malvern particle size analyzer (Zetasizer Nano ZSE, UK). Polypropylene gel electrophoresis experiment was performed on gel electrophoresis apparatus (JUNYI Electrophoresis, CN). Ultrapure water ($\geq$18.2 MΩ cm) was obtained from the water purification system (PALL, USA). The photo of the stained gel was captured by a camera (Panasonic LUMIX GF9, JP).

2.2. Materials and reagents

DNA and miRNA oligonucleotides used in the article were synthesized by Sangon Biotechnology Co., Ltd. (Shanghai, CN) and their sequences were listed in Table 1. Silver nitrate ($AgNO_3$), sodium borohydride ($NaBH_4$), Sodium chloride (NaCl), Magnesium chloride ($MgCl_2$), Phosphate salts ($Na_2HPO_4 \cdot 12H_2O$ and $NaH_2PO_4 \cdot 2H_2O$) and other reagents were purchased from Sinopharm Chemical Reagent Co., Ltd. (Shanghai, CN).

2.3. Detection of disease-related nucleic acids

For disease-related nucleic acids detection, single-stranded probe DNA1 (P1 or H1), DNA2 (P2 or H2) and the targets (miR-362 or hDNA) were dissolved in reaction buffer (20 mM $Na_2HPO_4 \cdot 12H_2O$ -$NaH_2PO_4 \cdot 2H_2O$, 20 mM NaCl, 2.5 mM $MgCl_2$, pH 7.0), respectively. For miR-362 assay, 10 μL of P1 (20 μM), 10 μL of P2 (20 μM) and 5 μL of miR-362 with different concentrations were mixed together, they were incubated at 25 °C for 30 min and then cooled slowly to 0 °C. Subsequently, 1.6 μL of $AgNO_3$ solution (1 mM) was added to the mixed solution and incubated for 30 min at 0 °C. A freshly prepared aqueous solution of $NaBH_4$ (1 mM) was added to the mixture, followed by vigorous shaking for 40 s. The resulting mixture was stored in dark at 0 °C for 2 h. The resulting NC probe solution with the molar ratio of NC probe DNA: Ag^+: $NaBH_4$ was 1: 8: 4. Finally, the fluorescent intensity was measured by a fluorescence spectrophotometer. All experiments were repeated 3 times. The detection method was also suitable for hDNA assay.

2.4. Native polyacrylamide gel electrophoresis

Native polyacrylamide gel electrophoresis was adopted to demonstrate the reaction between oligonucleotides as we designed. Firstly, the polyacrylamide gel was prepared from a mixed solution containing 20% acrylamide, 0.07% ammonium persulfate, 0.07% tetramethylethylene diamine and TBE buffer (89 mM

Table 1
Names and sequences of oligonucleotides.

Name	Sequence (5'-3')	Length(nt)
P1	TGAATCCTTGACCCGTTTT	19
P2	CCCCACCCCTATAGGTGTGTT	21
miR-362	AACACACCUAUUCAAGGAUUCA	22
M1-1	AACA<u>**T**</u>ACCTATTCAAGGATTCA	22
M1-2	AACACACCTATTCAAG<u>**A**</u>ATTCA	22
M2	AACA<u>**T**</u>ACCTATTCAAG<u>**A**</u>ATTCA	22
M3	AACA<u>**T**</u>A<u>**T**</u>CTATTCAAG<u>**A**</u>ATTCA	22
miR-223-3p	UGUCAGUUUGUCAAAUACCCCA	22
miR-let-7a	UGAGGUAGUAGGUUGUAUAGUU	22
miR-21	UAGCUUAUCAGACUGAUGUUGA	22
miR-155	UUAAUGCUAAUCGUGAUAGGGGU	23
H1	AGTCAGTGTGGACCCGTTTT	20
H2	CCCCACCCCTAAATCTCTAGC	21
hDNA	GCTAGAGATTTTCCACACTGACT	23
T1-1	GCTA<u>**T**</u>AGATTTTCCACACTGACT	23
T1-2	GCTAG<u>**G**</u>GATTTTCCACACTGACT	23
T2	GCTAG<u>**G**</u>GATTTTCCACA<u>**T**</u>TGACT	23
T3	GCTA<u>**T**</u>A<u>**A**</u>ATTTTCCACA<u>**T**</u>TGACT	23
HBV	AGTTACTCTCTTTTTTGCCTTCTGA	25
HTLA-1	GAGTATTTGCGCATGGCCTGGAGGA	25

The fragment pair of the Ag NC scaffold were marked in red and green in two DNA probes respectively (P1 and P2 were used to target miR-362; H1 and H2 were used to target hDNA). M1-1, M1-2, M2, and M3 were the one base, two bases, and three bases mismatch oligonucleotides of miR-362, respectively. T1-1, T1-2, T2, and T3 were the one base, two bases, and three bases mismatch oligonucleotides of hDNA, respectively. The mismatched sites were marked with underlines.

Tris, 89 mM boric acid and 2 mM EDTA). Then, oligonucleotide samples with volume of 10 μL containing 1 μL of loading buffer were added to the gel. Electrophoresis was performed in TBE buffer at 110 V for 2.5 h at room temperature. The gel was stained with $AgNO_3$ according to the followed steps: after fixation in 10% ethanol for 10 min, the gel was placed in 0.1% of $AgNO_3$ and shaken for 5 min, then washed by ultrapure water for 3 times followed by coloration with a mixture of 1.2% of NaOH and 0.4% of formaldehyde until clear bands appeared. Finally, the photo of the stained gel was captured by a camera.

3. Results and discussion

3.1. Construction of the method for disease-related nucleic acid detection

In this work, we designed two single-strand probe sequences, DNA1 and DNA2, which both were partially complementary to different parts of the same target, and contained a different split fragment of the Ag NC scaffold at the end of the sequence. When target nucleic acid was present, the ternary complexes of DNA1/DNA2/target would be formed through base pairing and compelled two split Ag NC fragments close to each other. As a result, a bright Ag NC with green emission would be produced at the assembled scaffold (C_4AC_4T/C_3GT_4) when $AgNO_3$ and $NaBH_4$ were both present. The scheme of target nucleic acids detection based on split DNA-Ag NC was illustrated in Fig. 1.

3.2. Feasibility of the method

To verify the formation of DNA1/DNA2/target ternary complex as we hypothesized, non-denaturing polyacrylamide gel electrophoresis was performed to analyze the interaction between nucleic acids. As shown in Fig. 2A, the results indicated that oligonucleotides with different components were showed different electrophoretic bands. Lane 1, lane 2 and lane 4 represented single-strand

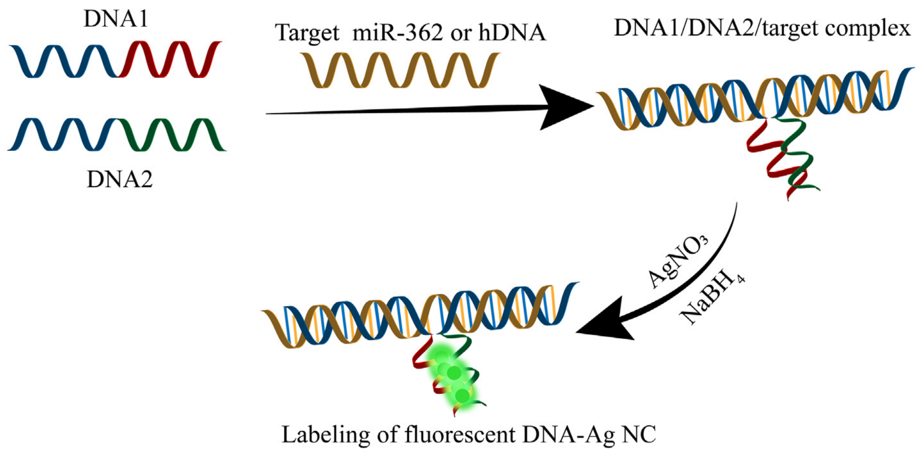

Fig. 1. The scheme of target miR-362 or hDNA detection based on labeling fluorescent Ag NC on a split DNA scaffold.

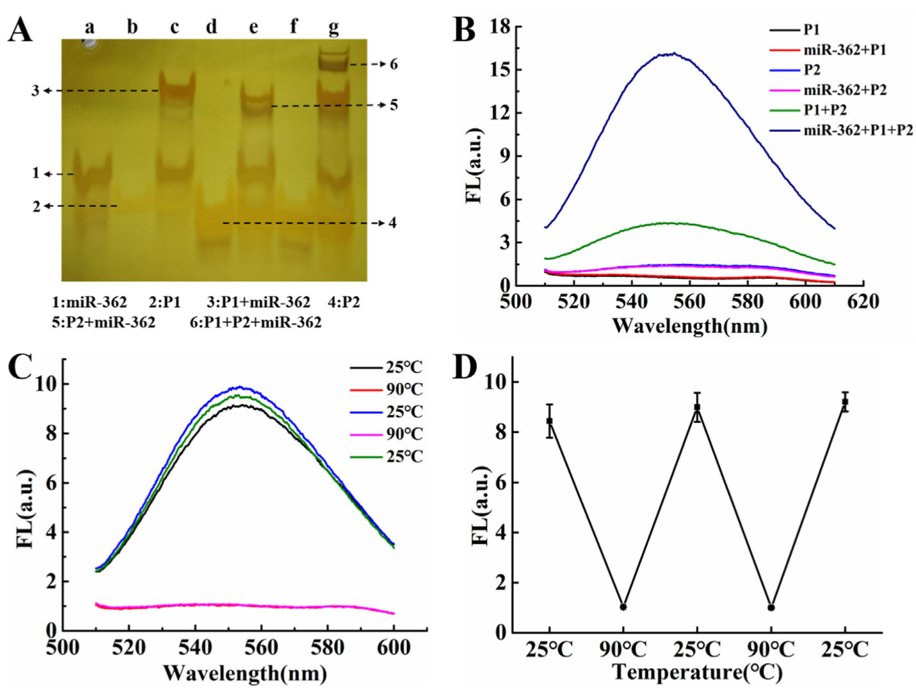

Fig. 2. Feasibility analysis of miR-362 detection. (A) Polyacrylamide gel electrophoresis to characterize oligonucleotides in different conditions (a: miR-362, b: P1, c: miR-362 + P1, d: P2, e: miR-362 + P2, f: P1+P2, g: miR-362 + P1+P2). The concentrations of nucleic acids were all 500 nM. (B) Fluorescence spectra of oligonucleotides with different components after incubation with $AgNO_3$ and $NaBH_4$ at the same conditions. (C) and (D) Changes in the fluorescence intensity of Ag NC formed by the P1/P2/miR-362 complex during a thermal cycling process. The concentrations of all nucleic acids were all 200 nM.

nucleic acids of miR-362, P1 and P2, respectively. Lane 3 and Lane 5 which were on behalf of the formation of P1/miR-362 and P2/miR-362 duplexes migrated slower than those of single-strand nucleotide acids. When P1, P2 and miR-362 were all present in this system, as shown in line 6, the migration was the slowest, indicating a ternary complex of P1/P2/miR-362 was formed. To investigate the target induced the formation of fluorescent Ag NC, fluorescence spectra of different components after incubation with $AgNO_3$ and $NaBH_4$ were obtained. As shown in Fig. 2B, neither single strand probe DNA (P1, P2) nor duplex complexes (P1/P2, P1/miR-362, P2/miR-362) could generate fluorescent Ag NC. Only when the target nucleic acids, P1 and P2 were present together, the strong fluorescence signal was detected, indicating fluorescent Ag NC only formed on the assembled Ag NC scaffold of the P1/P2/miR-362 ternary complex. A similar enhancement phenomenon of target hDNA was also observed and showed in Fig. S1. Furthermore, measurements of the fluorescence of the Ag NC developed by P1/P2/miR-362 complex during thermal cycling process (Fig. 2C and D) provided additional verification that the green fluorescence came from an assembled split-DNA Ag NC and demonstrated the reversibility of the fluorescence labeling mechanism. And the good stability of the DNA-Ag NC at room temperature (Fig. S3) indicated an excellent assay accuracy for target would be achieved with this probe. Taken together, these results proved that the proposed target-triggered labeling of fluorescent DNA-Ag NC platform for disease-related nucleic acid detection was feasible.

3.3. Characterization of DNA-Ag NC

As shown in Fig. 3A, the maximum excitation and emission wavelengths of the synthesized DNA-Ag NC were at 490 nm and 555 nm, respectively. The DNA-Ag NC exhibited green emission under UV light excitation (Fig. 3A, inset). The High-resolution transmission electron microscope (HRTEM) image demonstrated

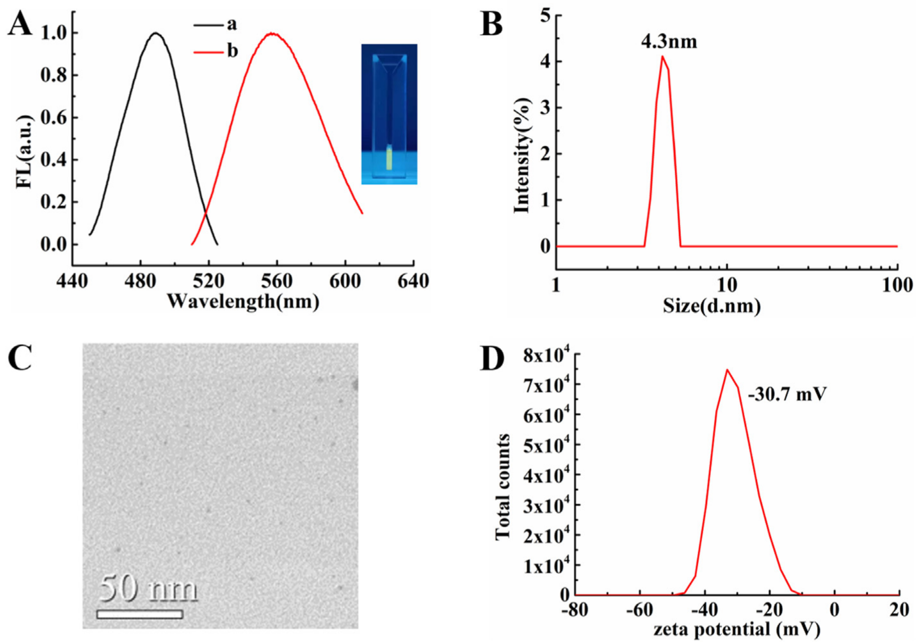

Fig. 3. Characterization of fluorescent DNA-Ag NC. (A) Excitation (a) and emission (b) spectra of synthesized DNA-Ag NC. Inset: Photograph of the synthesized silver cluster under UV irradiation. (C) TEM image of the prepared DNA-Ag NC. Dynamic Light Scattering measurement of the size (B), and Zeta Potential (D) of DNA-Ag NC.

that the synthesized DNA-Ag NC were uniform with a diameter of 3.0 nm (Fig. 3C). The DNA-Ag NC was also tested by dynamic light scattering (DLS) with a hydrodynamic size of 4.3 ± 0.5 nm and a size potential of −30.7 ± 0.5 mV (Fig. 3B and D). The hydraulic diameter of DNA-Ag NC by DLS was slightly larger than the result of TEM owing to the presence of solvent media.

3.4. Analytical performance for miR-362

The analytical performance of the strategy for quantitative analysis of nucleic acids was investigated. Fig. 4A depicted the fluorescence signal in response to miR-362 with different concentrations. A gradual increase in fluorescence intensity was observed when the concentration of miR-362 increased. As shown in Fig. 4B, the fluorescent intensity was linearly dependent on the concentration of miR-362 in the range from 20 nM to 200 nM with a calibration equation of $FL = 4.37 + 0.06C$ ($R^2 = 0.9929$). Meanwhile, the limit of detection (LOD) of miR-362 was calculated to be 6.5 nM. In order to evaluate the selectivity of the sensing platform for the target nucleotides detection, one(M1-1 and M1-2), two(M2), and three-base(M3) mismatch distinguish ability (Fig. 4D) and response to other disturbing miRNAs (Fig. S5), such as miR-21, miR-223, miR-let-7a and miR-155 that are involved in IBD-related signaling pathways [35–39], at the same analyzing condition were investigated, respectively. The results showed the signal response induced by the target miR-362 had significant difference ($p < 0.001$) than that induced by mismatched oligonucleotides or interfering miRNAs. It was indicated that our approach could specifically identify miR-362 even distinguish oligonucleotides at one base mismatched level. As shown in Figs S4 and S6, the same excellent selectivity of the sensing platform for hDNA was also observed.

The analytical features for miR-362 detection of this work were compared with other reported nucleic acid detection methods. As listed in Table 2, the LOD of miR-362 was comparable to that obtained by other detection methods and exhibited excellent selectivity for target assay. In addition, this one-step fluorescence labeling sensing platform was more cost-effective and easier to operate without complicated reactions.

3.5. Recovery test of nucleic acid detection in human serum samples

Lastly, we further evaluated the detection ability of this strategy in human serum samples. A certain concentration of standard miR-362 or hDNA was spiked into 1% diluted human serum. As shown in Table 3, the obtained recovery values of miR-362 were between 74.7% and 92.8%. The obtained recovery values of hDNA were shown in Table S1. These results indicated the biosensor had a potential application for detecting targets in real clinical serum samples.

4. Conclusion

In summary, a general nucleic acids analytical method based on target triggered labeling of fluorescent C_4AC_4T/C_3GT_4/Ag NC was developed. The sensing strategy has been successfully applied to the detection of miR-362 or hDNA with high sensitivity, good selectivity and satisfactory recovery in practical serum samples. Compared with other oligonucleotides detection methods, this one-step fluorescence labeling sensing platform is more cost-effective and easier to operate. Furthermore, assembled split-DNA Ag NC fluorescence labeling mechanism was further verified. This proposed strategy might be a potential alternative technique for disease-associated nucleic acids detection in clinic.

CRediT authorship contribution statement

Zhenzhen Jia: Formal analysis, Data curation, Software, Writing – original draft. **Kangsheng Tu:** Resources. **Qiuran Xu:** Writing – review & editing. **Wenhui Gao:** Validation, Software. **Cui Liu:** Writing – review & editing. **Biyun Fang:** Conceptualization, Funding acquisition, Writing – review & editing. **Mingzhen Zhang:** Funding acquisition, Supervision, Project administration.

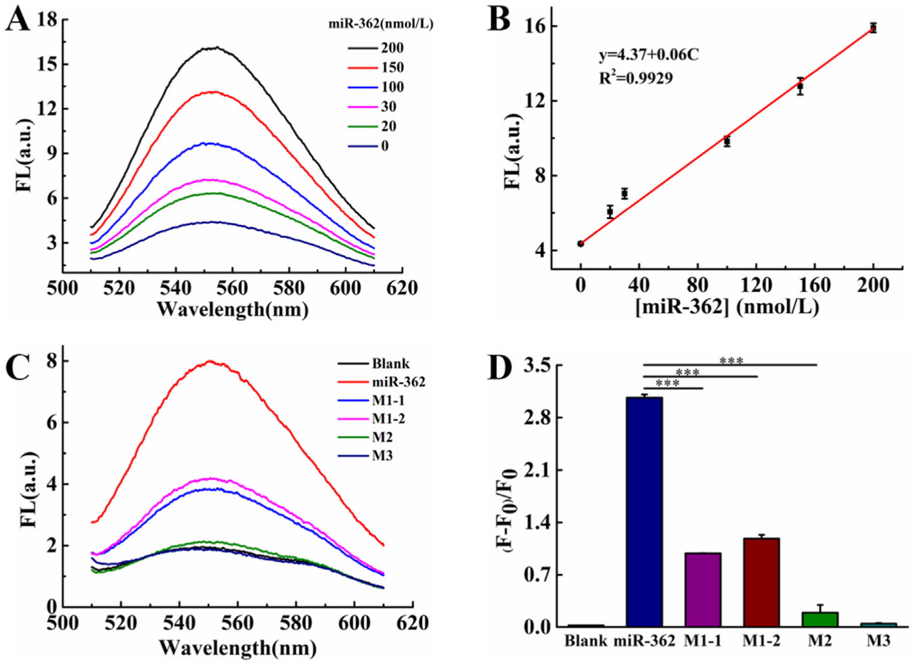

Fig. 4. Analytical performance of the sensing platform to miR-362. (A) Fluorescence response of the sensing platform to miR-362 with different concentrations (0–200 nM) and (B) Calibration curve of relative fluorescent intensity at 555 nm versus the concentration of miR-362. (C and D) Single, two, and three-base mismatch discrimination ability of the sensing platform. The concentrations of the base mismatched oligonucleotides and miR-362 were all 200 nM (n = 3). ***: $p < 0.001$.

Table 2
Comparison of the main characteristics for detection of oligonucleotides with other methods.

Target	Method	Detection limit	Range	Selectivity	References
miR-141	Colorimetry based on strand displacement reaction	0.48 nM	0–100 nM	miR-200b, miR-429, miR-21, let-7d	[12]
HIV DNA	Molecular beacon-based Ag NC	4.4 nM	10 –200 nM	One-base/two-base/four-base mismatched, absolutely mismatched target	[17]
miR-223	Strand displacement-based fluorescent Ag NC	28 nM	50 –450 nM	miR-155, miR-21, let-7a	[25]
miR-21	Graphene oxide/Ag NC hybrids-based fluorescent assay	Not mentioned	0 –1200 nM	One-base mismatched, noncomplementary sequence	[30]
Norovirus RNA	Target-triggered Ag NC synthesis	18 nM	20 –1800 nM	One-base/two-base/four-base/six-base/nine-base mismatched	[31]
H1N1	Molecular beacon-based activatable Ag NC	2 nM	10 –100 nM	One-base mismatched, random DNA	[28]
miR-362	Labeling of fluorescent Ag NC	6.5 nM	20 –200 nM	One-base/two-base/Three-base mismatched, miR-let-7a, miR-223, miR-21, miR-155	This work

Table 3
Recovery of miR-362 in human serum samples.

Sample	Spiked (n M)	Measured (n M)	Recovery (%)
1	150	130.9	87.3
		139.2	92.8
		129.4	86.2
2	150	112	74.7
		114.8	76.5
		146.9	98
3	150	121.58	81.1
		114.8	76.5
		125.58	83.7

Declaration of competing interest

The authors declare that they have no known competing financial interests or personal relationships that could have appeared to influence the work reported in this paper.

Acknowledgment

This work was supported by the National Natural Science Foundation of China (No. 82000523), the Natural Science Foundation of Shaanxi Province of China (Nos. 2020JQ-087, 2020JQ-095), the “Young Talent Support Plan” of Xi'an Jiaotong University, China (No. YX6J001), the Fundamental Research Funds for the Central Universities, China (No.xzy012019070), the China Postdoctoral Science Foundation, China (Nos. 2019M663657, 2020M683449). We also thank the Instrument Analysis Center of Xi'an Jiaotong University for the assistance with TEM and DLS analysis.

Appendix A. Supplementary data

Supplementary data to this article can be found online at https://doi.org/10.1016/j.aca.2021.338734.

References

[1] Y. Zhao, X. Zuo, Q. Li, F. Chen, Y.-R. Chen, J. Deng, D. Han, C. Hao, F. Huang, Y. Huang, G. Ke, H. Kuang, F. Li, J. Li, M. Li, N. Li, Z. Lin, D. Liu, J. Liu, L. Liu, X. Liu, C. Lu, F. Luo, X. Mao, J. Sun, B. Tang, F. Wang, J. Wang, L. Wang, S. Wang, L. Wu, Z.-S. Wu, F. Xia, C. Xu, Y. Yang, B.-F. Yuan, Q. Yuan, C. Zhang, Z. Zhu, C. Yang, X.-B. Zhang, H. Yang, W. Tan, C. Fan, Nucleic acids analysis, Sci. China Chem. 64 (2021) 171–203.

[2] C.K. Raymond, B.S. Roberts, P. Garrett-Engele, L.P. Lim, J.M. Johnson, Simple, quantitative primer-extension PCR assay for direct monitoring of microRNAs and short-interfering RNAs, RNA 11 (2005) 1737–1744.

[3] S.W. Kim, Z. Li, P.S. Moore, A.P. Monaghan, Y. Chang, M. Nichols, B. John, A sensitive non-radioactive northern blot method to detect small RNAs, Nucleic Acids Res. 38 (2010) 1–7.

[4] Q. Xiao, L. Yan, L. Yao, J. Lei, Z. Bi, J. Hu, Y. Chen, A. Fang, H. Li, Y. Li, Y. Yan, J. Zhou, Development of oligonucleotide microarray for accurate and simultaneous detection of avian respiratory viral diseases, BMC Vet. Res. 15 (2019) 253.

[5] S. Campuzano, M. Pedrero, J.M. Pingarron, Viral protein-based bioanalytical tools for small RNA biosensing, Trends Anal. Chem. 79 (2016) 335–343.

[6] Q.F. Xu, F. Ma, S.Q. Huang, B. Tang, C.Y. Zhang, Nucleic acid amplification-free bioluminescent detection of MicroRNAs with high sensitivity and accuracy based on controlled target degradation, Anal. Chem. 89 (2017) 7077–7083.

[7] H. Zhang, X. Xu, W. Jiang, An interparticle relatively motional DNA walker and its sensing application, Chem. Sci. 11 (2020) 7415–7423.

[8] C. Tao, Y. Yan, H. Xiang, D. Zhu, W. Cheng, H. Ju, S. Ding, A new mode for highly sensitive and specific detection of DNA based on exonuclease III-assisted target recycling amplification and mismatched catalytic hairpin assembly, Chem. Commun. 51 (2015) 4220–4222.

[9] E. Yang, D. Li, P. Yin, Q. Xie, Y. Li, Q. Lin, Y. Duan, A novel surface-enhanced Raman scattering (SERS) strategy for ultrasensitive detection of bacteria based on three-dimensional (3D) DNA walker, Biosens. Bioelectron. 172 (2021) 112758.

[10] M. Hou, D. He, H. Bu, H. Wang, J. Huang, J. Gu, R. Wu, H.W. Li, X. He, K. Wang, A sandwich-type surface-enhanced Raman scattering sensor using dual aptamers and gold nanoparticles for the detection of tumor extracellular vesicles, Analyst 145 (2020) 6232–6236.

[11] J. Zhou, L. Han, Y. Ling, L. Wang, N.B. Li, H.Q. Luo, A visual detection of human immunodeficiency virus gene using ratiometric method enabled by phenol red and target-induced catalytic hairpin assembly, Talanta 219 (2020) 121202.

[12] Y. Park, C.Y. Lee, S. Kang, H. Kim, K.S. Park, H.G. Park, Universal, colorimetric microRNA detection strategy based on target-catalyzed toehold-mediated strand displacement reaction, Nanotechnology 29 (2018), 085501.

[13] B.Y. Fang, C. Li, J. An, S.D. Zhao, Z.Y. Zhuang, Y.D. Zhao, Y.X. Zhang, HIV-related DNA detection through switching on hybridized quenched fluorescent DNA-Ag nanoclusters, Nanoscale 10 (2018) 5532–5538.

[14] Y. Jiang, P. Miao, DNA Dumbbell and Chameleon silver nanoclusters for miRNA logic operations, Research 2020 (2020), 1091605.

[15] Y. Jiang, X. Ma, X. Shao, M. Wang, Y. Jiang, P. Miao, Chameleon silver nanoclusters for ratiometric sensing of miRNA, Sensor. Actuator. B Chem. 297 (2019), 126788.

[16] J. He, Y. Zhang, Z. Chen, C. Li, R. Yuan, W. Xu, Targeted DNA-driven catalytic assembly light-up ratiometric fluorescence of biemissive silver nanoclusters for amplified biosensing, Chem. Commun. 56 (2020) 10325–10328.

[17] Q. Cao, Y. Teng, X. Yang, J. Wang, E. Wang, A label-free fluorescent molecular beacon based on DNA-Ag nanoclusters for the construction of versatile Biosensors, Biosens. Bioelectron. 74 (2015) 318–321.

[18] J.T. Petty, J. Zheng, N.V. Hud, R.M. Dickson, DNA-templated Ag nanocluster formation, J. Am. Chem. Soc. 126 (2004) 5207–5212.

[19] B. Han, E. Wang, Oligonucleotide-stabilized fluorescent silver nanoclusters for sensitive detection of biothiols in biological fluids, Biosens. Bioelectron. 26 (2011) 2585–2589.

[20] H.C. Yeh, J. Sharma, J.J. Han, J.S. Martinez, J.H. Werner, A DNA–silver nanocluster probe that fluoresces upon hybridization, Nano Lett. 10 (2010) 3106–3110.

[21] J.T. Petty, C. Fan, S.P. Story, B. Sengupta, A.S. Iyer, Z. Prudowsky, R.M. Dickson, DNA encapsulation of ten silver atoms produces a bright, modulatable, near infrared-emitting cluster, J. Phys. Chem. Lett. 1 (2010) 2524–2529.

[22] S. Huang, H. Yao, W. Wang, J.R. Zhang, J.J. Zhu, Highly sensitive fluorescence quantification of intracellular telomerase activity by repeat G-rich DNA enhanced silver nanoclusters, J. Mater. Chem. B 6 (2018) 4583–4591.

[23] J. Zhang, Y. Liu, X. Zhi, C. Zhang, T.F. Liu, D. Cui, DNA-templated silver nanoclusters locate microRNAs in the nuclei of gastric cancer cells, Nanoscale 10 (2018) 11079–11090.

[24] B. Fang, P. Guo, M. Yang, Y. Ma, X. Yan, Z. Jia, W. Gao, S. Ahmad, C. Xu, C. Liu, M. Zhang, A novel fluorescent enhancing platform based on DNA-scaffolded silver nanoclusters for potential inflammatory bowel disease-associated microRNA detection, Talanta 218 (2020) 121122.

[25] S.T. Lee, D. Beaumont, X.D. Su, K. Muthoosamy, S. Y, New, Formulation of DNA chimera templates: effects on emission behavior of silver nanoclusters and sensing, Anal. Chim. Acta 1010 (2018) 62–68.

[26] S.T. Lee, R. Rahman, K. Muthoosamy, N.A.H. Mohamed, X. Su, S. Tayyab, S. Y, New, Amplification-free and direct fluorometric determination of telomerase activity in cell lysates using chimeric DNA-templated silver nanoclusters, Microchim. Acta. 186 (2019) 81.

[27] G. Liu, J. Li, D.Q. Feng, J.J. Zhu, W. Wang, Silver nanoclusters beacon as stimuli-responsive versatile platform for multiplex DNAs detection and aptamer-substrate complexes sensing, Anal. Chem. 89 (2017) 1002–1008.

[28] B. Zhang, C. Wei, Highly sensitive and selective detection of $Pb(^{2+})$ using a turn-on fluorescent aptamer DNA silver nanoclusters sensor, Talanta 182 (2018) 125–130.

[29] K. He, R. Liao, C. Cai, C. Liang, C. Liu, X. Chen, Y-shaped probe for convenient and label-free detection of microRNA-21 in vitro, Anal. Biochem. 499 (2016) 8–14.

[30] F. Shen, Y. Cheng, Y. Xie, H. Yu, W. Yao, H.W. Li, Y. Guo, H. Qian, DNA-silver nanocluster probe for norovirus RNA detection based on changes in secondary structure of nucleic acids, Anal. Biochem. 583 (2019) 113365.

[31] C. He, P.M. Goodwin, A.I. Yunus, R.M. Dickson, J.T. Petty, A split DNA scaffold for a green fluorescent silver cluster, J. Phys. Chem. C 123 (2019) 17588–17597.

[32] A. Omidbakhsh, M. Saeedi, M. Khoshnia, A. Marjani, S. Hakimi, Micro-RNAs -106a and -362-3p in peripheral blood of inflammatory bowel disease patients, Open Biochem. J. 12 (2018) 78–86.

[33] F. Wu, N.J. Guo, H. Tian, M. Marohn, S. Gearhart, T.M. Bayless, S.R. Brant, J.H. Kwon, Peripheral blood microRNAs distinguish active ulcerative colitis and Crohn's disease, Inflamm. Bowel Dis. 17 (2011) 241–250.

[34] C. Rouzioux, P. Tremeaux, V. Avettand-Fenoel, HIV DNA: a clinical marker of HIV reservoirs, Curr. Opin. HIV AIDS 13 (2018) 389–394.

[35] B. Cao, X. Zhou, J. Ma, W. Zhou, W. Yang, D. Fan, L. Hong, Role of MiRNAs in inflammatory bowel disease, Dig. Dis. Sci. 62 (2017) 1426–1438.

[36] H.Y. Kim, H.Y. Kwon, H.T. Ha Thi, H.J. Lee, G.I. Kim, K.B. Hahm, S. Hong, MicroRNA-132 and microRNA-223 control positive feedback circuit by regulating FOXO3a in inflammatory bowel disease, J. Gastroenterol. Hepatol. 31 (2016) 1727–1735.

[37] M. De Robertis, M.L. Poeta, E. Signori, V.M. Fazio, Current understanding and clinical utility of miRNAs regulation of colon cancer stem cells, Semin. Canc. Biol. 53 (2018) 232–247.

[38] M. Altaf-Ul-Amin, M.B. Karim, P. Hu, N. Ono, S. Kanaya, Discovery of inflammatory bowel disease-associated miRNAs using a novel bipartite clustering approach, BMC Med. Genom. 13 (2020) 10.

[39] Y. Feng, Y. Zhang, D. Zhou, G. Chen, N. Li, MicroRNAs, intestinal inflammatory and tumor, Bioorg. Med. Chem. Lett 29 (2019) 2051–2058.